IEEE Access
Multidisciplinary ⋮ Rapid Review ⋮ Open Access Journal

Received March 21, 2022, accepted April 20, 2022, date of publication April 26, 2022, date of current version May 11, 2022.

Digital Object Identifier 10.1109/ACCESS.2022.3170462

Study on Internal Strain Distribution of the High-Field Nb_3Sn Superconducting Accelerator Magnets With Homogenization Theory

ZHEN ZHANG AND QINGJIN XU

Laboratory of Particle Acceleration Physics and Technology, Institute of High Energy Physics, Chinese Academy of Sciences, Beijing 100049, China
University of Chinese Academy of Sciences, Beijing 100049, China

Corresponding author: Qingjin Xu (xuqj@ihep.ac.cn)

This work was supported in part by the Strategic Priority Research Program of the Chinese Academy of Sciences (CAS) under Grant XDB25000000, and in part by the National Key Research and Development Program of China under Grant 2018YFA0704200.

ABSTRACT To fabricate 10-16 Tesla high-field accelerator magnets, the high-Jc Nb_3Sn superconductor is one of the most practical choices. However, it is a brittle material and is strain-sensitive. To reduce the potential Jc degradation of the conductor, it is crucial to accurately evaluate the stress of the coils owing to the large Lorentz force during magnet excitation. In the traditional stress analysis of magnets, the coils are usually regarded as homogenized structures using isotropic material coefficients; however, most superconducting (SC) coils have hierarchical and complicated structures. To obtain a more accurate estimation, it is necessary to consider the detailed internal structure of the coils during stress analysis. In this study, the homogenization method was applied to multi-scale stress analysis of a high-field accelerator SC magnet. The effective material coefficients of Nb_3Sn coils were calculated using this method. Stress analysis of the magnet was performed using the effective material coefficients and isotropic material coefficients for comparison. Compared with the result obtained using isotropic material coefficients, the Von-Mises stress of the coil using effective material coefficients is larger at different load steps. The stress level of most Nb_3Sn filaments in the strand was higher than that of the coil. The maximum stress of the Nb_3Sn filaments appeared in the strand contact regions. In addition, there was a significant difference in the average stress of all materials in the strand. These findings will help develop more accurate analysis and simulation models for high-field SC magnets.

INDEX TERMS Homogenization method, Nb_3Sn, stress analysis, superconducting magnet.

I. INTRODUCTION

Stress control is essential for the design and fabrication of high-field SC magnets. On the one hand, the SC materials used to fabricate the high-field SC coils, such as Nb_3Sn, are stress-sensitive; on the other hand, the coils in the magnet sustain a large electromagnetic force during excitation. Presently, in the stress simulation of an SC magnet, the coil is regarded as a whole without an internal microstructure, and the material of the coils is regarded as an isotropic material. The material properties of the coil were obtained through experimental tests. However, the coils are complicated heterogeneous and hierarchical composites, including five scales, from a single SC filament to a full coil [1]. In addition, in a quench analysis of the magnet, it was found that the degradation of some coils was due to the fracture of filaments in the strand caused by excessive prestress [2]. Therefore, it is necessary to evaluate the stress of coils with internal microstructures. Usually, it is difficult to calculate the stress distribution of a magnet directly with these detailed microstructures in traditional methods, even with advanced computers.

Multi-scale analysis methods [1], [3]–[9] are appropriate solutions for the above problem. Multiple researchers [7], [9] have developed multi-scale models to study the mechanical behavior of Nb_3Sn material between the strand and filament levels. The homogenization method [1], [4]–[6] is one such method, which can take into account micro-scale information at the macro-scale. The stress distribution in the composites can be accurately calculated using the effective

The associate editor coordinating the review of this manuscript and approving it for publication was Jingang Jiang.

coefficients with the homogenized structure. This method has been applied to calculate the effective coefficients of a variety of composites. It has also been used in the analysis of SC coils for nuclear fusion devices, and the simulation results are in good agreement with experimental results [5].

In this study, for the first time, the homogenization method has been applied to the stress analysis of an accelerator SC magnet, to study the mechanical behavior of Nb_3Sn material between the magnet and filament levels. First, the related theory is introduced, and the effective material coefficient and stress recovery formulas are given. Secondly, based on the actual SC strand structure inside the SC coil, the homogenization finite element model of the strand is built, and effective material coefficients are calculated. Finally, a stress analysis of the SC magnet named LPF1 developed at IHEP [10], [11] is performed, which simulates three load steps: magnet assembly, cool down and excitation with effective material coefficients and isotropic material coefficients. The stress in the filament and strand is recovered and discussed based on the simulation results for the magnet during excitation.

II. BRIEF REVIEW OF THE HOMOGENIZATION THEORY

The homogenization theory developed in the 1970s was a limit theory [12]–[14]. In theory, asymptotic expansion and periodic assumptions are used to simplify differential equations. For some specific equations, the solutions are almost equivalent to those of the initial equation [15]. The macro-scale and micro-scale properties of the composites can be predicted using this theory. The following is a brief introduction to the basic concepts and formulas. The detailed derivation is described in [1], [4]–[6].

Here, two different scales are considered: one is the macro-scale x representing the composite, and the other is the micro-scale y representing the cell of periodicity of the composite Y. The ratio of the actual sizes of the two scales is the characteristic inhomogeneity dimension ε, which is a very small value. In this way, the material properties inside the composite are piecewise uniform [1].

$$D_{ijkl}(x+Y) = D_{ijkl}(x); y = \frac{x}{\varepsilon} \tag{1}$$

where D is the Y-periodic fourth-order elastic tensor of the material. The governing equations are as follows:

$$\sigma_{ij}^{\varepsilon}(x,y) = D_{ijkl}(y)\, e_{kl}^{\varepsilon} - D_{ijkl}(y)\alpha_{kl}(y)\,\theta^{\varepsilon} \tag{2}$$

$$\sigma_{ij}(x,y) = D_{ijkl}^{H} e_{kl}(x) - D_{ijkl}^{H}\alpha_{kl}^{H}\theta(x) \tag{3}$$

where superscript ε indicates that the problem is based on the characteristic inhomogeneity dimension, and superscript H represents the homogenization values. The meaning of the other symbols is that σ is the stress tensor, e is the strain tensor, α is the coefficient of thermal expansion, and θ is the temperature. When ε is close to be zero, Eqs. (3) becomes a limit form of Eqs. (2). The stress and strain in the equation depend on macro-variables and satisfy the general equilibrium equation. The new constitutive equation contains the effective material coefficient, which ensures the energy conservation of the equation [1].

$$u^{\varepsilon}(x) = u^{0}(x) + \varepsilon u^{1}(x,y) + o\left(\varepsilon^{2}\right) \tag{4}$$

For Eqs. (2), the displacement is expressed by the double-scale asymptotic expansion, as shown in Eqs. (4). u is the displacement tensor. The first-order component represents the macro-displacement field, and the second-order component represents the micro-displacement disturbance. Then, the first-order and second-order displacement are solved using the volume average and global integral. Finally, the effective elastic modulus, effective coefficient of thermal expansion, and local stress recovery formulas are obtained, as shown in Eqs. (5)-(7).

$$D_{ijkl}^{H}(x) = \frac{1}{|Y|}\int_{Y}\left(D_{ijkl}(y) - D_{ijpq}(y)\frac{\partial \chi_{p}^{kl}}{\partial y_{q}}\right)dY;\ \chi_{i}^{pq} \in V_{Y} \tag{5}$$

$$\alpha_{ij}^{H}(x) = \left[D_{ijkl}^{H}\right]^{-1}\frac{1}{|Y|}\int_{Y}\left(\alpha_{ij}(y) - \alpha_{kl}(y)\frac{\partial \chi_{p}^{kl}}{\partial y_{q}}\right)dY \tag{6}$$

$$\sigma_{ij}^{0}(y) = \left(D_{ijkl}(y) - D_{ijpq}(y)\frac{\partial \chi_{p}^{kl}}{\partial y_{q}}\right)e_{kl}(x) - \left(D_{ijkl}(y)\alpha_{kl}(y) - D_{ijpq}(y)\alpha_{kl}(y)\frac{\partial \chi_{p}^{kl}}{\partial y_{q}}\right)\cdot\theta^{0}(x) \tag{7}$$

where χ is the displacement homogenization equation of the cell of periodicity. By solving these equations, the effective elastic modulus, effective coefficient of thermal expansion, and local stress of the material can be solved. Based on the above equation and the finite element software, a homogenization finite element program has been developed, and then the effective coefficient and local stress can be solved by the program.

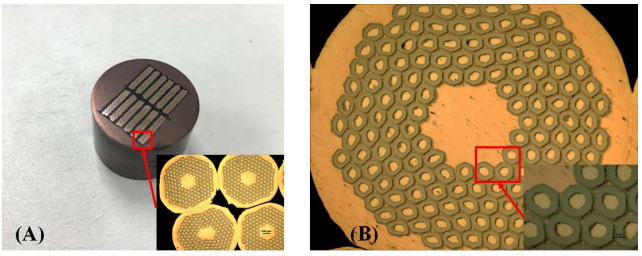

FIGURE 1. (A) The image of the coil segment and (B) The optical image of the strand.

III. HOMOGENIZATION MODEL TO STUDY THE HIGH FIELD ACCELERATOR MAGNETS

A. THE CHARACTERIZATION OF THE SC STRAND FOR ACCELERATOR SC MAGNETS

As stated, the SC coils are the above composite with a periodic structure, which is composed of strands and

epoxy resin. Here, the macro-scale is the coil and the micro-scale is the strand. The homogenization method can be applied to calculate the effective coefficient of the coil. The effective coefficients mean the effective elastic modulus and effective coefficient of thermal expansion. The cell of periodicity is an impregnated strand.

To build a homogenization finite element model, it is necessary to obtain the geometric structure of the strand. In this study, a tested Nb_3Sn SC coil was used as the experimental sample to obtain the geometric dimensions of the strand. First, the straight part of the coil was cut into coil segments. Then, the coil segment was made into the strand stack sample. The cross-section of the sample was mechanically polished using SiC pads. The grit size of the pad ranges from 320 to 1200. Then it was polished using diamond slurries of particle size (5μm, 3μm). Finally, the sample was characterized using an optical microscope. The optical image of the strand is shown in Fig. 1. The geometric dimensions of the internal structures of the strand are listed in Table 1.

TABLE 1. Strand geometric specification.

Quantity	Value
Type of conductor	RRP
No.Of filaments	144/169
Strand diameters, mm	0.85
Nb hexagon apothem, μm	27.5
Sn rod radius, μm	13.81
Cu spacing, μm	4.7

B. THE CALCULATION OF EFFECTIVE MATERIAL COEFFICIENTS

Based on the geometric dimensions, a homogenization finite model of the strand was built, as shown in Fig. 2. This model contains all microstructures of the strand, including the epoxy resin, OHFC Cu matrix, Nb_3Sn filaments, and Sn rods.

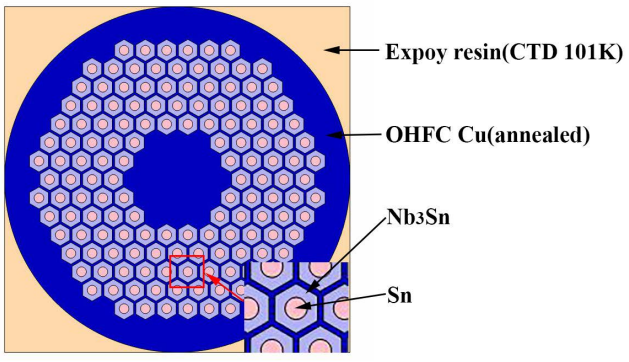

FIGURE 2. Geometric cross-section of the impregnated strand.

The properties of all materials in the impregnated strand are listed in Table 2 [16], [17]. After the geometric model was built, periodic boundary conditions were applied to the opposite sides of the model. The prestress load derived from homogenization theory was applied to all domains of the model. The homogenization model was obtained and the homogenization equations were solved. The effective elastic modulus and effective coefficient of thermal expansion were calculated with the equations.

TABLE 2. Materials properties.

Material	E, GPa	ν	α, 10^{-6} / K
Epoxy resin (CTD 101K)	2.4	0.4	50
Nb_3Sn	125	0.37	7
OHFC Cu (annealed)	118	0.36	17
Sn	41.4	0.33	17

TABLE 3. Effective material properties.

Quantity	Value
D_{11}, GPa	56.8
D_{12}, GPa	21.2
D_{22}, GPa	57.0
D_{66}, GPa	14.2
α_{11}, 10^{-6}/K	16.15
α_{22}, 10^{-6}/K	16.18

TABLE 4. Isotropic material properties.

Quantity	Value
Young's modulus, GPa	35
Poisson ratio	0.3
Coefficient of thermal expansion, 10^{-6} / K	11.6

Table 3 lists the components of the effective elastic modulus and the effective coefficient of thermal expansion. Note that the subscript representation of the effective elastic modulus adopts the Voigt notation. The non-zero components of the material coefficients are listed. The components that are not listed are zero. Besides, the isotropic material coefficients of the Nb_3Sn coil are listed in Table 4.

C. THE STRESS ANALYSIS OF THE SC MAGNET AND THE STRAND

Stress analysis of an accelerator SC magnet named LPF1 was performed. In this analysis, the stress in the central Nb_3Sn coil was calculated with effective material coefficients and isotropic material coefficients respectively. The results were compared and discussed. Based on the symmetrical structure of the magnet, a 1/4 2D finite element model is built to calculate the stress distribution of the magnet. The cross-section of the magnet is shown in Fig. 3. The magnet is composed of two Nb_3Sn coils and four NbTi coils. The detailed

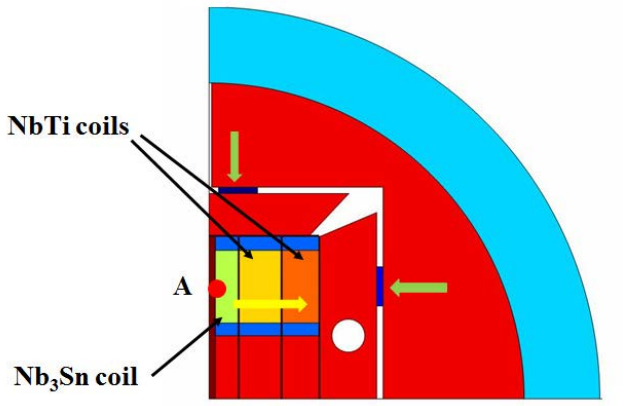

FIGURE 3. Geometric cross-section of LPF1, a 10-Tesla model dipole magnet with Nb_3Sn and NbTi coils [10], [11]. The yellow arrow represents the main direction of electromagnetic force. The green arrows represent the main direction of prestress.

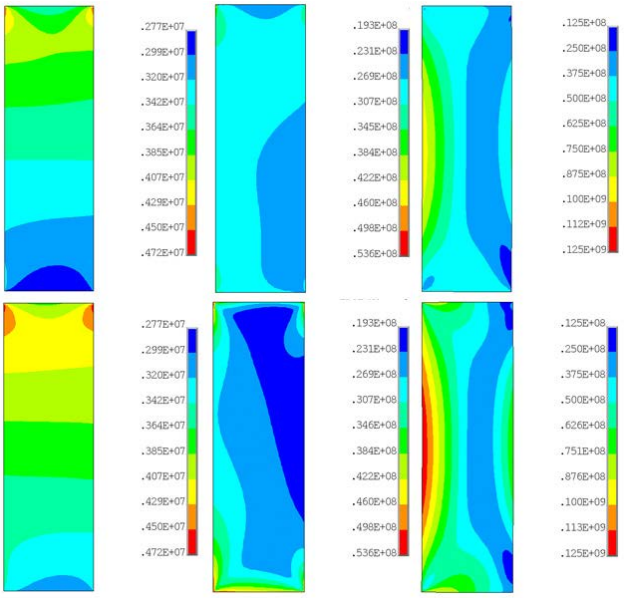

FIGURE 4. Von-Mises stress in the Nb_3Sn coil at different load steps with effective material coefficients and isotropic material coefficients. From left to right: Von-Mises stress in the Nb_3Sn coil after the assembly, cool down, and excitation; from the top to bottom: isotropic material coefficients and effective material coefficients.

mechanical structure and design of the magnet are described in [10], [11]. The stress simulations of the magnet include three load steps: assembly, cool down, and magnet excitation. By using the above simulation, the stress components at point A of the Nb_3Sn coil were obtained during the excitation. Point A was located at the middle of the straight part of the Nb_3Sn coil, where the highest field is located. Then the stress distribution of the strand at point A was recovered with the homogenization method.

IV. RESULTS AND DISCUSSION

The Von-Mises stress of the Nb_3Sn coil using effective material coefficients and isotropic material coefficients at different load steps are shown in Fig. 4. At the step of the magnet assembly, the stress distribution and maximum Von-Mises stress in the coil using different material coefficients shows a little difference, as shown in Fig. 4 left column. After the cool down and excitation, the difference becomes more and more significant. The maximum Von-Mises stress or strain calculated by using the effective material coefficients is larger than the value calculated with the isotropic material coefficients. The discrepancy in maximum Von-Mises stress or strain during the excitation is larger than that at the other load steps. It shows that the different material coefficients have a relatively large impact on the maximum Von-Mises stress or strain evaluation in the coil during the magnet excitation.

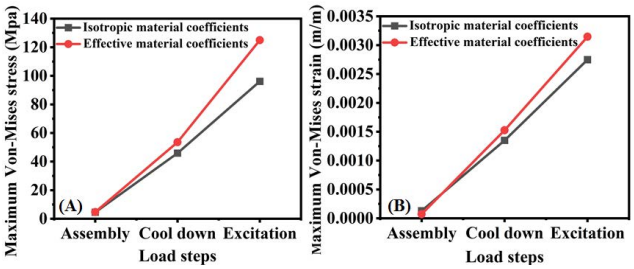

FIGURE 5. (A) Maximum Von-Mises stress and (B) Maximum Von-Mises strain in the Nb_3Sn coil at different load steps with effective material coefficients and isotropic material coefficients.

In addition, compared with the maximum Von-Mises strain, the discrepancy in the maximum Von-Mises stress is relatively larger during excitation. In a traditional way of a study model, the maximum Von-Mises stress is used to evaluate the current-carrying capacity of the coil, the coil performance would be greatly overestimated in such type of model. Furthermore, the discrepancy between the maximum and average Von-Mises stress in the Nb_3Sn coil is shown in Fig. 6. It also becomes more and more significant after the cool down and excitation using effective material coefficients. It shows that the stress distribution in the coil is more uneven after cool down and excitation. The overall stress of the coil is low but the local stress is high. Since the effective material coefficients are closer to the actual material coefficients, which reflects more accurately the actual mechanical behavior of materials. The maximum Von-Mises stress and the stress distribution are essential in the stress analysis of the magnet. Evaluating them accurately could better optimize the design of the magnet.

The strain and stress components of the coil at point A are obtained from the simulation results at the excitation. The strain components ε_{xx}, ε_{yy}, and ε_{xy} are -3.75×10^{-3}, -7.16×10^{-3}, and -5.86×10^{-6} respectively. The stress components σ_{xx}, σ_{yy}, and σ_{xy} are -0.954 MPa, -122.55 MPa, and -0.095 MPa respectively. With the strain components, the stress of the strand at this point was recovered. The stress distributions of the filaments inside the strand are shown in Fig. 7. It shows that the distribution of each stress component is quite different and the stress range is large. There are both tensile stress and compressive stress

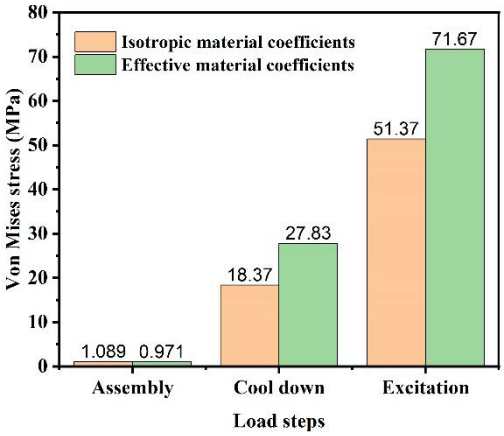

FIGURE 6. The discrepancy between the maximum and average Von-Mises stress in the Nb_3Sn coil at different load steps with effective material coefficients and isotropic material coefficients.

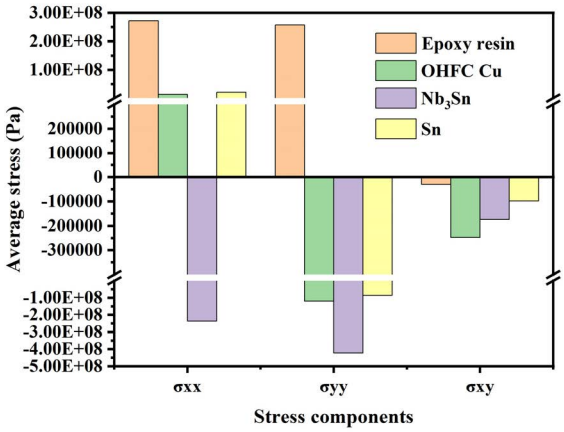

FIGURE 8. Average stress of stress components σ_{xx}, σ_{yy}, and σ_{xy} of all materials in the impregnated strand.

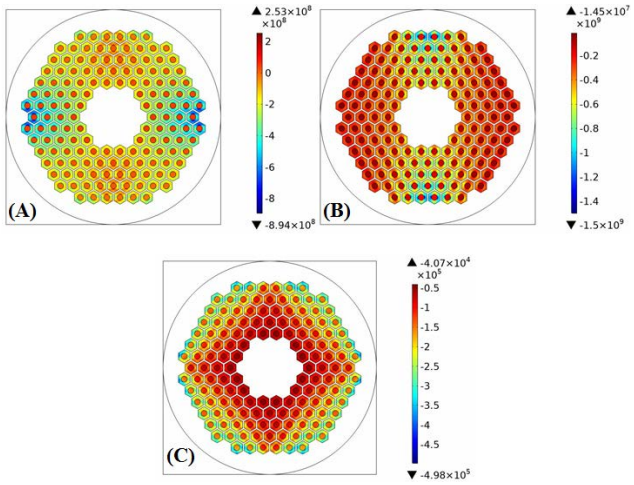

FIGURE 7. Stress distributions of the filaments inside the strand at point A of the Nb_3Sn coil. Stress components (a) σ_{xx}, (b) σ_{yy}, and (c) σ_{xy}.

in the Nb_3Sn filaments. The stress of most Nb_3Sn filaments is at the same level, however, the stress of a few filaments at the edge of the strand is significantly larger than the other parts, possibly because it is the contact region between adjacent strands. This phenomenon was also observed in [3]. Considering the stress and strain sensitive nature of the high-field superconductors like Nb_3Sn, it indicates that the current-carrying capacity of these filaments will degrade first when the stress level of the strand is high. The Maximum stress appears in the conjunction of the Nb_3Sn filament and the Sn rod. Because the material properties of the Nb_3Sn filaments are different from that of Sn rods. Thus, stress evaluation for the SC material will help us better understand the mechanical behavior of the SC material.

The difference in the average stresses of all materials of the impregnated strand is significant as shown in Fig. 8. Stress component σ_{xx} of epoxy resin, OHFC Cu, and Sn are tensile stress, but that of Nb_3Sn is compressive stress. Note that stress component σ_{xx} at the macro-scale level is compressive. It indicates that the stress state of the materials in the strand is quite different from that of the coil. Meanwhile, the average stress of stress components σ_{xx} and σ_{yy} of the epoxy resin are larger. Epoxy resin will be cracked by high stress, which may become the origin of the quench. Stress evaluation of all materials will help find the origin of the quench. Furthermore, the stress level in the Nb_3Sn filaments is much larger than that in the coil at point A.

Because the stress in the other materials is lower than that in the filaments. Meanwhile, the stress at the macro-scale level is the average stress of the strand. In addition, the average stress of Nb_3Sn is larger in all materials. The volume proportion of Nb_3Sn in the strand is the largest. So, the stress state of Nb_3Sn determines the stress state of the coil at the point A. In conclusion, the mechanical behavior of all materials inside the coil will directly affect the performance of the coil. An accurate stress evaluation of these materials will help to optimize the stress distribution in the SC strands and coils, to further improve the performance of the coil and avoid some quench origins.

V. CONCLUSION

In this study, a study model was developed for the multi-scale stress analysis of the accelerator SC magnets by applying the homogenization theory. An Nb_3Sn coil was cut open to make a strand block to obtain the geometric dimension of the strand for building the homogenization finite model. The effective material coefficients of the coil were calculated from the model. The stress analysis of the magnet was performed using different material coefficients. The results show that at the macro-scale, the maximum Von-Mises stress in the coil at three load steps using effective material coefficients is higher than that using isotropic material coefficients. The distribution of Von-Mises stress of the coil is more uneven using effective material coefficients. At the micro-scale, all stress components of the impregnated strand in the coil were recovered. The stress state, stress level, and stress distribution

of all materials in the impregnated strand are obtained. This information will help us more accurately evaluate the stress state of the Nb_3Sn filaments. It will also help the SC conductor and magnet designers to optimize the stress distribution in the SC strands and coils to further improve their performance.

REFERENCES

[1] B. Hassani and E. Hinton, "A review of homogenization and topology optimization I—Homogenization theory for media with periodic structure," *Comput. Struct.*, vol. 69, no. 6, pp. 707–717, Dec. 1998.
[2] S. Balachandran, J. Cooper, O. B. Van Oss, P. J. Lee, L. Bottura, A. Devred, F. Savary, C. Scheuerlein, and F. Wolf, "Metallographic analysis of 11 T dipole coils for high luminosity-large hadron collider (HL-LHC)," *Supercond. Sci. Technol.*, vol. 34, no. 2, Feb. 2021, Art. no. 025001.
[3] M. Daly, C. H. Loffler, D. Smekens, A. T. Fontenla, O. S. de Frutos, M. Guinchard, and F. Savary, "Multiscale approach to the mechanical behavior of epoxy impregnated Nb_3Sn coils for the 11 T dipole," *IEEE Trans. Appl. Supercond.*, vol. 28, no. 3, pp. 1–6, Apr. 2018.
[4] B. Hassani and E. Hinton, "A review of homogenization and topology opimization II—Analytical and numerical solution of homogenization equations," *Comput. Struct.*, vol. 69, no. 6, pp. 719–738, Dec. 1998.
[5] M. Lefik and B. A. Schrefler, "Application of the homogenisation method to the analysis of superconducting coils," *Fusion Eng. Des.*, vol. 24, no. 3, pp. 231–255, Jun. 1994.
[6] D. P. Boso, M. Lefik, and B. A. Schrefler, "A multilevel homogenised model for superconducting strand thermomechanics," *Cryogenics*, vol. 45, no. 4, pp. 259–271, Apr. 2005.
[7] D. Arbelaez, S. O. Prestemon, P. Ferracin, A. Godeke, D. R. Dietderich, and G. Sabbi, "Cable deformation simulation and a hierarchical framework for Nb_3Sn Rutherford cables," *J. Phys., Conf. Ser.*, vol. 234, no. 2, Jun. 2010, Art. no. 022002.
[8] N. Mitchell, "Finite element simulations of elasto-plastic processes in Nb_3Sn strands," *Cryogenics*, vol. 45, no. 7, pp. 501–515, Jul. 2005.
[9] D. P. Boso, M. Lefik, and B. A. Schrefler, "Multiscale analysis of the influence of the triplet helicoidal geometry on the strain state of a Nb_3Sn based strand for ITER coils," *Cryogenics*, vol. 45, no. 9, pp. 589–605, Sep. 2005.
[10] C. Wang, D. Cheng, K. Zhang, Y. Wang, E. Kong, Z. Zhang, S. Wei, L. Gong, Z. Zhang, Q. Peng, X. Yang, H. Liu, Y. Tan, T. Zhao, Y. Zhu, Y. Zhao, H. Liao, Z. Zhu, F. Chen, and Q. Xu, "Electromagnetic design, fabrication, and test of LPF1: A 10.2-T common-coil dipole magnet with graded coil configuration," *IEEE Trans. Appl. Supercond.*, vol. 29, no. 7, pp. 1–7, Oct. 2019.
[11] K. Zhang, Y. Wang, C. Wang, D. Cheng, E. Kong, Q. Peng, Z. Zhang, S. Wei, X. Yang, and Q. Xu, "Mechanical design, assembly, and test of LPF1: A 10.2 T Nb_3Sn common-coil dipole magnet with graded coil configuration," *IEEE Trans. Appl. Supercond.*, vol. 29, no. 4, pp. 1–8, Jun. 2019.
[12] É. Sanchez-Palencia, *Non-Homogeneous Media and Vibration Theory* (Lecture Notes in Physics), vol. 127, 1980.
[13] G. Papanicolau, A. Bensoussan, and J.-L. Lions, *Asymptotic Analysis for Periodic Structures*, 1978.
[14] D. Cioranescu and J. S. J. Paulin, "Homogenization in open sets with holes," *J. Math. Anal. Appl.*, vol. 71, no. 2, pp. 590–607, Oct. 1979.
[15] O. OA, "On homogenization problems," in *Trends and Application of Pure Mathematics in Mechanics*, 1984.
[16] E. Barzi, C. Franceschelli, I. Novitski, F. Sartori, and A. V. Zlobin, "Measurements and modeling of mechanical properties of Nb_3Sn strands, cables, and coils," *IEEE Trans. Appl. Supercond.*, vol. 29, no. 5, pp. 1–8, Aug. 2019.
[17] C. Scheuerlein, B. Fedelich, P. Alknes, G. Arnau, R. Bjoerstad, and B. Bordini, "Elastic anisotropy in multifilament Nb_3Sn superconducting wires," *IEEE Trans. Appl. Supercond.*, vol. 25, no. 3, pp. 1–5, Jul. 2015.

ZHEN ZHANG received the B.S. degree from the Nanjing University of Science and Technology, in 2017. He is currently pursuing the Ph.D. degree with the Laboratory of Particle Acceleration Physics and Technology, Institute of High Energy Physics, Chinese Academy of Sciences. His research interests include stress measurement and control of superconducting magnets.

QINGJIN XU received the Ph.D. degree from the Graduate University of the Chinese Academy of Sciences, in 2006. From 2003 to 2007, he participated in the development of the first superconducting particle detector magnet in China: BESIII detector magnet. From 2008 to 2014, he worked at the High Energy Accelerator Research Organization (KEK, Tsukuba, Japan) and European Nuclear Research Organization (CERN, Geneva, Switzerland) on the advanced superconducting magnet research and development for the HL-LHC Project. Since March 2014, he moved back to the Institute of High Energy Physics (IHEP), leading the advanced superconducting magnet research and development for future high energy accelerators. He is currently the Head of the Superconducting Magnet Group, IHEP, Chinese Academy of Sciences (CAS).